Purdue University

Purdue e-Pubs

International Refrigeration and Air Conditioning Conference

School of Mechanical Engineering

2014

Extremum Seeking Control of Hybrid Ground Source Heat Pump System

Bin Hu
University of Texas at Dallas, United States of America, bxh140030@gmail.com

Yaoyu Li
University of Texas at Dallas, United States of America, yaoyu.li@utdallas.edu

Baojie Mu
University of Texas at Dallas, United States of America, Baojie.Mu@utdallas.edu

Shaojie Wang
Climate Master, Inc., Oklahoma City, OK 73179, USA, wsjsxn@gmail.com

John E. Seem
High Altitude Trading, Inc., Jackson, WY 83001, US, john.seem@gmail.com

See next page for additional authors

Follow this and additional works at: http://docs.lib.purdue.edu/iracc

Authors

Bin Hu, Yaoyu Li, Baojie Mu, Shaojie Wang, John E. Seem, and Feng Cao

Extremum Seeking Control of Hybrid Ground Source Heat Pump System

Bin Hu[1,2], Yaoyu Li[1*], Baojie Mu[1], Shaojie Wang[3], John E. Seem[4], Feng Cao[2]

[1]Department of Mechanical Engineering, University of Texas at Dallas,
Richardson, TX 75080, USA

[2]School of Energy and Power Engineering, Xi'an Jiaotong University,
Xi'an, 710049, China

[3]Climate Master, Inc., Oklahoma City, OK 73179, USA

[4]High Altitude Trading, Inc. Jackson, WY 83001, USA

*Corresponding Author
Tel: (972) 883-4698; Fax: (972) 883-4659; E-mail address: yxl115230@utdallas.edu

ABSTRACT

The Hybrid Ground Source Heat Pump (GSHP) system features the combination of ground heat exchanger (GHE) and cooling tower for rejecting the cooling load, which enables the use of the renewable resource of geothermal energy while reducing the cost of installation for applications of high cooling demand. However, model based control for efficient operation of the GSHP system can be intricate due to variations in ambient conditions and equipment characteristics, as well as the cost, accuracy and reliability of sensors required. In this study, a nearly model-free self-optimizing control strategy is proposed for the efficient operation for GSHP based on the Extremum Seeking Control (ESC) scheme. The proposed ESC scheme is based on the feedback of the total power consumption of heat pump compressor, cooling tower fan, and water pump of ground loop and the control inputs are cooling tower relative flow rate. The heat pump is controlled with an inner-loop proportional-integral (PI) controller to regulate the evaporator0 leaving water at 7°C. The proposed control strategy is simulated on a Modelica based dynamic simulation model. The vertical GHE model is adopted from the Buildings Library developed by Lawrence Berkeley National Laboratories (LBNL), for which the transient heat transfer process is implemented with the finite volume method inside and outside the borehole. Simulation was conducted for a small office building in Dallas area under two scenarios: one is a change in evaporator inlet water temperature (i.e. load change), and the other is a change in ambient air condition. The simulation results demonstrated the effectiveness of the proposed ESC strategy, and the potential for energy saving is also evaluated.

1. INTRODUCTION

The ground source heat pump (GSHP) technology is a renewable alternative for space conditioning by rejecting/absorbing heat to/from the ground, which has demonstrated higher energy efficiency for residential and commercial buildings. After the first oil crisis in 1970s, GSHP systems have thrived in North America and Europe for energy saving and environmental protection [1]. It is well known that the GSHP systems can achieve better energy performance in specific locations where building heating and cooling loads demonstrate year-around balance due to the long-term transient heat transfer in the ground heat exchanger (GHE). However, a lot of commercial buildings are cooling-dominated with unbalanced loads, especially those located in warm-climate areas. Under such circumstance, much more heat is rejected into the ground than that absorbed from the ground, causing heat accumulation in the ground. Such heat accumulation results in increase of the ground temperature and then higher temperature of water entering the heat pump and performance degradation of the GSHP system accordingly [2]. This problem may be solved by increasing the total capacity of GHE, however, the system capacity is limited by the initial cost of construction. Therefore, developing the so-called hybrid GSHP system by utilizing supplemental heat rejecters such as cooling tower (as shown in Figure 1) has emerged as a cost-effective alternative.
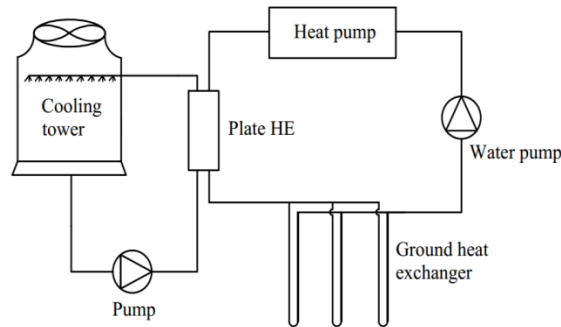
Figure 1: Schematic diagram of typical hybrid GSHP System

There have been extensive studies on the design strategies of the hybrid GSHP systems, as reviewed in Alavy *et al.* [3]. For example, Caneta Research [4] and Kavanaugh and Rafferty [5] presented design approaches for cooling-dominant buildings that would require longer GHE to meet the total cooling demand rather than the total heating demand, and also made the prediction for the capacity of the GSHP systems. Kavanaugh [6] revised and extended these design procedures for cooling tower design in hybrid systems. Chiasson [7] investigated the optimal control and operating strategies for the annual thermal load balance in the ground and optimized the ground loop length and cooling tower capacity based on simulation. For a heating-dominant building, Ni *et al.* [8] presented a brute-force approach to find the optimal design ratio for a GSHP with a gas boiler as the auxiliary heat source.

Various simulation-based approaches have also been studied in the simulation and analysis of optimal control and operation of hybrid GSHP systems for cooling-dominated applications. Caneta Research [4] indicated the advantages of hybrid GSHP systems in warm-climate areas considering initial costs and available surface area limitations. Yavuzturk and Spitler [9, 10] investigated the advantages and disadvantages of various control strategies for a hybrid GSHP system with a cooling tower under different climatic conditions. A series of operating strategies for the cooling tower and various night-time schedules at various times of the year were examined. Ramamoorthy *et al.* [11] used a system simulation approach to finding the optimal size of a supplemental cooling with a GHP system serving a cooling-dominated office building. For a system with both space conditioning and water heating requirement, Wrobel [12] presented a parameter estimation scheme for the hybrid GSHP design. Using the physics-based models of the hybrid GSHP system in TRNSYS, Hackel [13] proposed a simulation based design optimization algorithm which minimizes the life-cycle cost for cooling-dominated applications. Man *et al.* [14] developed an hourly simulation model of the hybrid GSHP system with a cooling tower in order to model and analyze the heat transfer processes of its main components. Some operational strategies are also investigated for a sample building.

Most existing methods for control and optimization of hybrid GSHP system operation have been based on nominal/empirical models. In practice, due to uncertain changes in cooling load and hard-to-estimate system degradation, such models may often be inaccurate. Therefore, real-time setpoint optimization not replying on exact system knowledge is more desirable for operations of the hybrid GSHP systems. The Extremum Seeking Control (ESC) has recently emerged as a major class of self-optimizing control strategies, in which the gradient estimation is carried out by a dither-demodulating scheme. As a dynamic realization of gradient search, ESC can search for the optimal input in real time in a nearly model-free fashion [15-17]. ESC has recently drawn significant attention for HVAC applications. Li *et al.* [18] and Li *et al.* [19] presented ESC schemes for efficient operation of the air-side economizer and chilled-water systems, respectively.

In this study, an ESC based control scheme is proposed to achieve efficient operation of the hybrid GSHP system in real time. The ESC scheme is based on the feedback of the total power for the heat pump compressor, the tower fan and the water pump, and the control inputs are the tower fan speed and the condensing water flow rate. To evaluate the proposed control strategy, a Modelica [20] based dynamic simulation model is developed for a hybrid GSHP system in Dymola [21]. The proposed system diagram of ESC working on hybrid GSHP system is illustrated in the schematic in Figure 2.
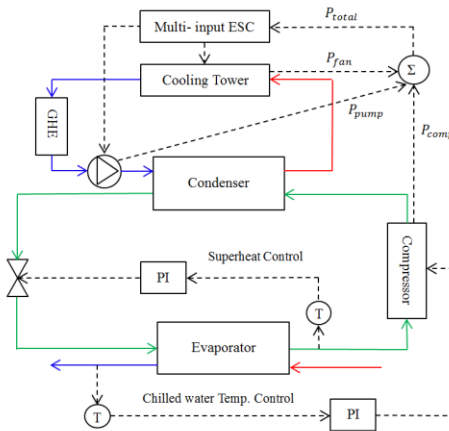
Figure 2: Basic system diagram of ESC working on hybrid GSHP system

The remainder of this paper is organized as follows. The dynamic models of GHE are presented first, followed by the models of other components of the hybrid GSHP system. The ESC framework and design procedure are briefly reviewed. Finally, the simulation study is presented to validate the proposed method.

2. GROUND-LOOP HEAT EXCHANGER MODEL

In practical applications, the heat transfer process in a GHE involves a number of uncertain factors, such as ground thermal properties, soil constituents, ground water fraction, and building loads over a long lifespan of several or even tens of years. For operation of such systems, the heat transfer process should be treated as transient. In view of the complexity of GHE, the associated heat transfer process is analyzed in two separated parts in this study. One is the part inside the borehole, including the grout, the U-tube pipes and the circulating fluid inside the pipes. This part is analyzed as being steady-state or quasi-steady-state. The other part is the solid soil/rock outside the borehole, where the heat conduction must be treated as a transient process. The temperature distribution varies with time and distance from the borehole center. The cylindrical source model developed in Modelica Buildings Library version 1.5 [21] is adopted to determine the fluid temperature, which is circulated in the U-tubes and the heat pump, under certain operating conditions.

2.1 Quasi -three-dimensional model
The heat flows per unit length for two pipes are denoted as q_1 and q_2, respectively. Assuming the validity of linear superposition, the steady-state temperature is deemed as the sum of the temperature resulted from the two heat sources. Taking the average temperature of the borehole wall as reference yields the following equations [22, 23]:

$$T_{f1} - T_b = R_{11}q_1 + R_{12}q_2 \qquad (1a)$$

$$T_{f2} - T_b = R_{12}q_1 + R_{22}q_2 \qquad (1b)$$

R_{11} and R_{22} are the thermal resistances between the two pipes and borehole wall, respectively. R_{12} is the thermal resistance between the two pipes. T_b is the average temperature of the borehole wall. In practice, typical U-tube pipes have symmetric structure, therefore

$$R_{11} = R_{22} = \frac{1}{2\pi k_b}\left[\ln\frac{r_b}{r_p} + \sigma \cdot \ln\left(\frac{r_b^2}{r_b^2 - D^2}\right)\right] + R_p \qquad (2a)$$

$$R_{12} = \frac{1}{2\pi k_b}\left[\ln\frac{r_b}{2D} + \sigma \cdot \ln\left(\frac{r_b^2}{r_b^2 - D^2}\right)\right] \qquad (2b)$$

where $\sigma = \frac{k_b - k}{k_b + k}$ and $R_p = \frac{1}{2\pi k_p}\ln\frac{r_b}{r_{pi}} + \frac{1}{2\pi r_{pi}h}$ is the thermal resistances between the fluid and outer pipe wall. r_{pi} and r_p are the inner and outer radius of pipe, respectively. r_b is the radius of borehole and D is the half spacing of U-tube shanks. h is the convective heat transfer coefficient of the fluid and the inner wall of U-tube, k denotes the thermal conductivity of soil/rock around the borehole, while k_b and k_p are the thermal conductivity of grouting material and pipe material, respectively. The difference between the inlet and outlet temperatures of GHE is not large, usually

less than 10K, so physical parameters along the pipes (such as specific heat, density, etc.) are approximated constant. The heat conduction of the grout and ground in the axial direction is ignored. The heat flow rate can be expressed as:

$$q_1 = \frac{R_{12}(T_{f2}-T_b)-R_{11}(T_{f1}-T_b)}{R^2{}_{12}-R^2{}_{11}} \tag{3a}$$

$$q_2 = \frac{R_{12}(T_{f1}-T_b)-R_{11}(T_{f2}-T_b)}{R^2{}_{12}-R^2{}_{11}} \tag{3b}$$

In this model, the convective heat flow along the fluid channels is balanced by the conductive heat flows among the fluid channels and borehole wall. With this hypothesis, the energy equilibrium equation of the fluid in downward and upward pipes can be formulated as:

$$-MC_P \frac{dT_{f1}(z)}{dz} = \frac{R_{12}(T_{f2}(z)-T_b)-R_{11}(T_{f1}(z)-T_b)}{R^2{}_{12}-R^2{}_{11}} \tag{4a}$$

$$MC_P \frac{dT_{f2}(z)}{dz} = \frac{R_{12}(T_{f1}(z)-T_b)-R_{11}(T_{f2}(z)-T_b)}{R^2{}_{12}-R^2{}_{11}} \tag{4b}$$

The boundary conditions:

$$0 \leq z \leq H ; z = 0 , T_{f1} = T_{f,in} ; z = H , T_{f1} = T_{f2} \tag{5}$$

2.2 Cylindrical source model

The borehole heat exchanger, with vertical length of L_{Bor}, is vertically discretized into n elements of height $L=L_{Bor}/n$. For each segment, the transient conductive heat transfer in the borehole, in the soil and for the far-field boundary condition [24].

$$\rho c \left(\frac{\partial T(r,t)}{\partial t}\right) = k \left(\frac{\partial^2 T(r,t)}{\partial r^2} + \frac{1}{r}\frac{\partial T(r,t)}{\partial r}\right) \tag{6}$$

where ρ is the mass density, c is the specific heat capacity per unit mass, $T(r, t)$ is the temperature at radius r and time t, and k is the thermal conductivity of soil/rock around the borehole.

The boundary conditions:

$$-2\pi r_b k \left.\frac{\partial T(r,t)}{\partial r}\right|_{r=r_b} = q_1 \qquad \text{for } t \geq 0 \tag{7a}$$

$$T(t = 0) = T_0 \quad \text{for } r \gg r_b \tag{7b}$$

where r_b is the borehole radius.

3. HYBRID GSHP MODEL

The dynamic model of hybrid GSHP system is developed with Dymola 2014 [20] and Modelica Buildings Library 1.5 [21]. For this study, the dynamics of heat pump and cooling tower are much faster than that of GHE, so the static state models of heat pump and cooling tower are adopted. The hybrid GSHP system model consists of a 20-borehole GHE, a water-to-water heat pump, a counter-flow cooling tower and a plate heat exchanger. A variable-flow water pump model is constructed for the GHE water loop, which gives power consumption under different operating scenarios.

3.1 Cooling tower model

The York cooling tower model *Buildings.Fluid.HeatExchangers.CoolingTowers.YorkCalc* in the Modelica Buildings Library 1.5 [21] is adopted to compute the thermal performance of the cooling tower. This model takes as parameters the approach temperature, the range temperature and the inlet air wet bulb temperature at the design condition. The water flow rate is used as input to compute the heat transfer with water side of the cooling tower.

$$W_{tower} = C_{p,w} \cdot m_{w,nom} \cdot T_{ran} \tag{8}$$

where $C_{p,w}$ is the specific heat of water, $m_{w,nom}$ is the water mass flow rate at the nominal/designed condition, and T_{ran} is the range temperature, which is defined as the temperature difference between the entering water and exiting water for the cooling tower. The nominal fan power is sized to be 1.05% of the design load [25], i.e.

$$W_{fan} = 0.0105 \cdot W_{tower} = 0.0105 \cdot C_{p,w} \cdot T_{ran} \cdot m_{w,nom} \tag{9}$$

Based on the York data, the nominal power consumption of the fan is determined by:

$$P_{fan,nom} = fraP_{fan,nom} \cdot m_{w,nom} \tag{10}$$

$fraP_{fan,nom}$ [W/ (kg/s)] is defined as the fan power divided by the water mass flow rate at the nominal condition , with the default value being 275 Watts for a water flow rate of 0.15 kg/s [21]. For off-design conditions, the relative air flow rate FR_{air} and relative water flow rate FR_{wat} are introduced to get the cooling tower performance. The York Calculation is followed to compute the approach temperature for free convection and forced convection.

To regulate the cooling tower leaving water temperature at a setpoint value, a PI controller is implemented to adjust the relative air flow rate, and the corresponding fan power consumption is obtained. The output of the controller y (= FR_{air}) is the nominalized volume flow rate of the air (relative air flow rate). When $y < 0.3$, it is free convection heat transfer process and $P_{fan} = 0$. When $y \geq 0.3$ it is forced convection heat transfer process and the fan power can be determined by:

$$P_{fan} = y^3 \cdot fraP_{fan,nom} \cdot m_w \tag{11}$$

where y is the relative air flow rate, m_w is water mass flow rate $fraPfan,nom$ is the ratio of fan power and water mass flow rate with the default value 1833[W/ (kg/s)] [21].

3.2 Heat pump model

The performance of heat pump affects the efficiency and energy consumption of whole hybrid GSHP system. Therefore, a heat pump simulation model is needed to calculate the coefficient of performance (COP) and effusing fluid temperature of the heat pump according to its entering fluid temperature, and then the energy consumption of heat pump can be analyzed.

A simplified heat pump model is used to simulate the operation of whole hybrid GSHP system. The COP of this model changes with temperatures in the same way as the Carnot efficiency changes. The COP can be computed by the model based on the Carnot effectiveness, in which case

$$COP_0 = \eta_{car} COP_{car} = \eta_{car} \cdot \frac{T_{eva}}{T_{con} - T_{eva}} \tag{12}$$

where T_{eva} is the evaporator temperature, and T_{con} is the condenser temperature. η_{car} is the Carnot effectiveness. An inner-loop proportional-integral (PI) controller is implemented to regulate the evaporator leaving water temperature at 280.15K.

The water pump model is described to predict the power consumption by the pump. A pump model from *Buildings.Fluid.Movers.FlowMachine_Nrpm* has been adopted [21], with the pump affinity law defined similarly to that for the fan modeling.

4. EXTREMUM SEEKING CONTROL

The objective for ESC is to find the optimal input $u_{opt}(t)$ in real time for a generally unknown and/or time-varying performance function $f(t, u)$ with the online measurement of the objective value to be minimized [15], i.e.

$$u_{opt}(t) = \arg \min f(t, u) \tag{13}$$

where $u_{opt}(t)$ is the input vector. The nonlinear system with input-output performance function $f(t, u)$ is assumed to have a convex characteristic with a global minimum. The self-optimizing algorithms are designed to find the minimum value of the performance function. A typical dither ESC block diagram is shown in Figure 3. The transfer functions $F_I(s)$ and $F_O(s)$ denote the input dynamics and sensor dynamics, respectively. The output of the performance function $f(t, u)$ is assumed to be directly observable for feedback. The demodulation and signals dither are as follows:

$$d_1^T(t) = [\sin(\omega_1 t) \cdots \sin(w_m t)] \tag{14}$$

$$d_2^T(t) = [a_1 \sin(\omega_1 t + \alpha_1) \cdots a_m \sin(w_m t + \alpha_m)] \tag{15}$$

where ω_i and α_i are the frequency and phase angle, respectively. a_i is the dither amplitude. The dithered output signal passes through the high-pass filter $F_{HP}(s)$, multiplied by the demodulating signal $d_1(t)$ and low-pass filtered by $F_{LP}(s)$, resulting in a signal proportional to gradient $\partial f/\partial u$. Closed-loop integral control can make the gradient vanish if the closed-loop system is stable. The compensator $K(s)$ can be designed to enhance the transient performance or stability.
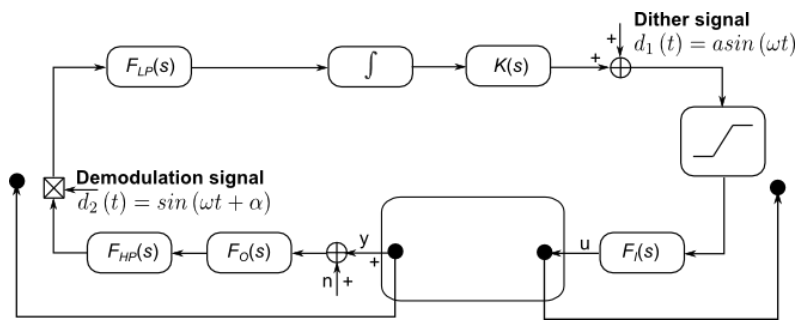

Figure 3: Block diagram of designed dither ESC

The design of a dither ESC needs to determine several components mentioned above: the dither signal $d(t)$, the high-pass filter $F_{HP}(s)$, the low-pass filter $F_{LP}(s)$, and the compensator $K(s)$. The detailed design method is introduced by Li [27]. In practical applications, all actuators have physical limitations, which saturate the control actions at certain point. The integral windup could be a problem for ESC system operations. Therefore integral windup could be a problem for ESC system operations. To avoid the integral windup, some anti-windup techniques have been proposed in the past [28, 29]. Li and Seem [30] proposed a back calculation based anti-windup strategy, which is compatible with the simple nature of extremum seeking control. In this study, this scheme is applied to deal with the possible integral windup due to relative air flow rate saturation.

5. SIMULATION RESULT AND DISCUSSION

In this study, the dither ESC control scheme is applied to the hybrid ground-source heat pump system to minimize the total power consumption of by regulating the relative air flow rate. In order to demonstrate the ESC for minimizing the total power consumption under different load conditions, the building load scenario described by Chiasson [7] has been adopted, in which a generic office building located in Dallas for cooling-dominated applications is presented. The modeled office building had a plan area of 1858m^2 in two floors with a rectangular floor plan. The hourly heating and cooling loads for the generic buildings follow those in [7].

Then the input dynamics is estimated based the slowest step response to achieve better robustness:

$$F_I(s) = \frac{5580 \cdot 0.001029^2}{s^2 + 2 \cdot 0.0179 \cdot 0.001029 \cdot s + 0.001029^2} \tag{16}$$

The cutoff frequency of the input dynamics ω_c is about 0.000827 rad/s. The dither frequency ω_{dis} selected as 0.0000628 rad/s. F$_{HP}$(s) and F$_{LP}$(s) are chosen as

$$F_{HP}(s) = \frac{s^2}{s^2 + 2 \cdot 1.11 \cdot 0.0000314 \cdot s + 0.0000314^2} \tag{17a}$$

$$F_{LP}(s) = \frac{0.0000314^2}{s^2 + 2 \cdot 1.11 \cdot 0.0000314 \cdot s + 0.0000314^2} \tag{17b}$$

The dither amplitude is selected as 0.02.

5.1 Fixed cooling load condition

The standard ESC performance is tested under fixed part-load operating conditions. The ambient wet-bulb temperature for the cooling-tower inlet air flow is set to be 296.15K. Under the full-load condition, the mass flow rate for the evaporator water loop is set to be 6kg/s, while the entering water temperature is set at 286.15K. The part-load operating conditions are simulated by adjusting the evaporator entering water temperature T_{EW}. Figure 4(a) shows the static map from relative air flow rate to the total power consumption under 80% cooling load (T_{EW} =284.95K), with the optimal relative air flow rate and power consumption estimated as 0.515 and 32.6kW, respectively.

The simulation first starts at a fixed relative air flow rate of 0.9, and the ESC controller is turned on at t = 500,000s. As shown in Figure 4(b), the ESC search results in the average steady-state relative air flow rate of 0.53 and the total power of 33.2kW, respectively, with the 1% settling time of about 731520s. Compared to the estimated optimum in the static map, the steady-state error is about 3.1% and 1.5% for the relative air flow rate and the total power, respectively. The ESC controller is then tested for 50% cooling load with the adjustment of the evaporator inlet water temperature T_{EW} from 284.95K to 283.15K.
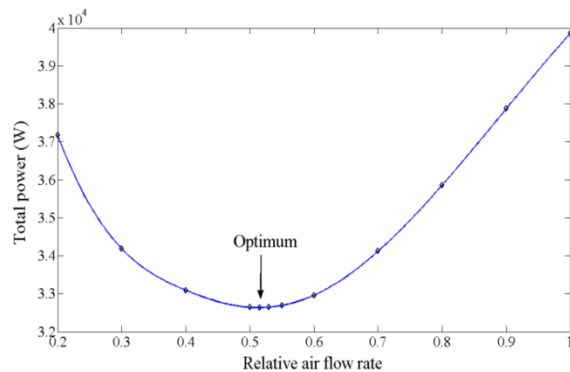

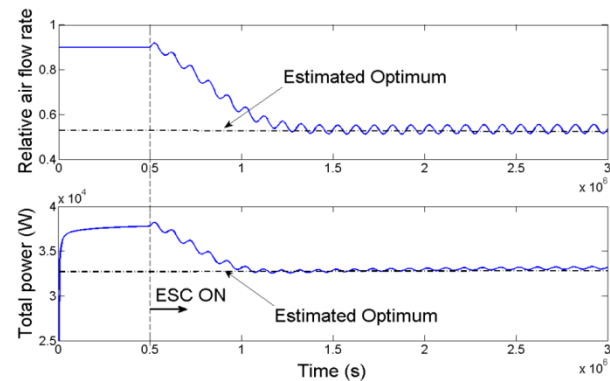**Figure 4(a)**: Static map under 80% cooling load

Figure 4(b): ESC simulation results for 80% cooling load

The other simulation condition is the same as the previous case of fixed cooling load conditions. The static map from relative air flow rate to the total power consumption for 50% cooling load is presented in Figure 5(a), with the optimal relative air flow rate is 0.412 and total power is 20.1kW. For the decrease of cooling load, the total power consumption of the whole hybrid GSHP decreases, correspondingly the optimal relative air flow rate decreases too.

As shown in Figure 5(b), the ESC searched average steady-state relative air flow rate and the total power of the second condition are about 0.425 and of 20.4kW, differing from the estimated optimum by only 2.9% and 1.6%, respectively. The power output settles within ±1% of its steady state is about 782,365s. Also, as marked in Figure 5(b), if the relative air flow rate remained at initial value of 0.9 during cooling load change, the system would consume 26.8kW. Therefore, dither ESC adapts the system operation with power saving of 6.4kW (23.8%).
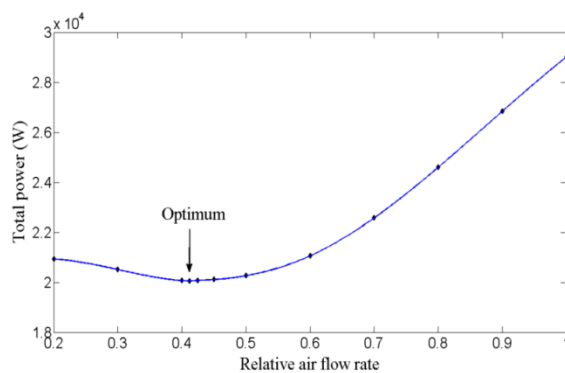

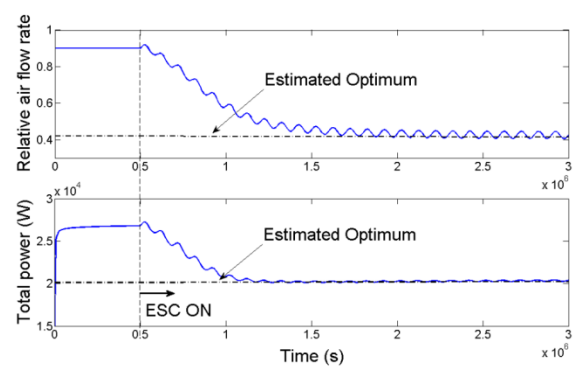**Figure 5(a)**: Static map under 50% cooling load

Figure 5(b): ESC simulation results for 50% cooling load

5.2 Variable cooling load conditions

Then the standard ESC controller is tested with a change in cooling load conditions by varying the evaporator inlet water temperature in the simulation. The ramp starts at t=2,000,000s, and lasts for 60s. The ambient wet-bulb temperature for the cooling-tower inlet air flow is also set as 296.15K. The ESC simulation results for 80% to 50% cooling load are shown in Figure 6(a), which shows the integral windup problem of the standard ESC with actuator saturation. In the upper subplot, the optimum is successfully achieved by ESC search before the ramp change. From 2,000,000s, under the change of system condition, the relative air flow rate is saturated at 1. The ESC fails to search for the new optimum due to the integral windup. The relative air flow rate is stuck at the saturation limit. The lower subplot of Figure 6(a) shows the cooling load variation by changing the evaporator inlet water temperature. Then, the back-calculation based anti-windup ESC scheme is applied to the same case above. As shown in Figure 6(b), the anti-windup ESC responds to the system condition change when the ramp change of T_{EW} starts and converges to the new optimum successfully. Compared to the results for standard ESC, the optimal searched relative air flow rate for anti-windup ESC is closed to static value. In this case, the system would consume 29.2kW. Therefore, anti-windup ESC adapts the system operation with power saving of 8.8kW (30.2%).
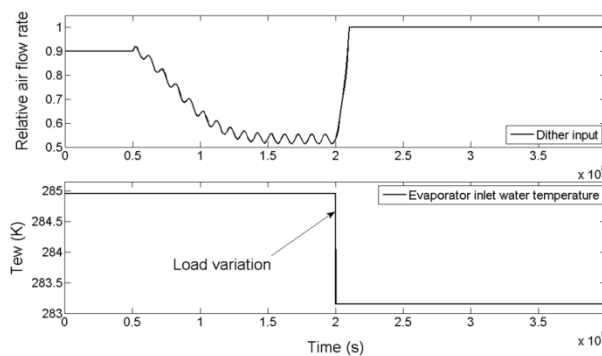

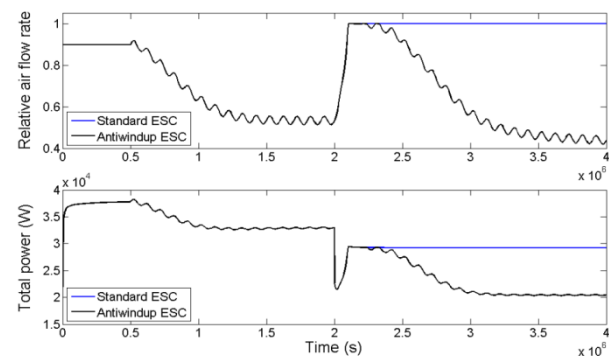**Figure 6(a)**: Standard ESC with actuator saturation   **Figure 6(b)**: Anti-windup ESC with actuator saturation

In summary, the proposed ESC scheme is validated with simulations on the detailed simulation model of hybrid GSHP system. It is noteworthy that the extremum seeking control does not rely on the knowledge of the plant models. Compared to the model based methods in the aforementioned literatures, this scheme does not rely on unreliable sensors or accurate process model, which makes the method much more robust to sensor failure and plant variation due to unknown environment changes and the hard-to-estimate system degradation. Also, the back-calculation based anti-windup ESC scheme can also handle the problem comes from actuator saturation.

6. CONCLUSION

This paper presents an ESC based hybrid GSHP control scheme which can minimize the combined power consumption of GHE loop water pump, cooling tower fan and pump, and heat pump compressor. The proposed ESC control strategy is tested on a dynamic simulation model of the hybrid GSHP system developed by utilizing the Buildings Library of the Lawrence Berkeley National Laboratory. The transient heat conduction model of vertical GHE is a combination of Quasi-three-dimensional model inside the borehole and cylindrical source model outside the borehole. A static polynomial cooling tower model based on a York cooling tower correlation is adopted to regulate the leaving water temperature and fan power consumption. The heat pump model is based on the evaporator temperature, condenser temperature and Carnot efficiency. An inner-loop proportional-integral (PI) controller is implemented to regulate the evaporator leaving water temperature at 280.15K.

Simulation study was performed for a scenario of fixed cooling load condition and then for varying cooling load conditions, in which ramp changes are introduced to the evaporator inlet water temperature. The ESC searched results show reasonable steady-state errors compared to the predicted static maps even under varying cooling load conditions. The power saving performance is also evaluated for the simulated examples with respect to the cooling tower relative air flow rate, which indicates about 23.8% power saving across the adjustable range of inputs. The effectiveness of the back-calculation based anti-windup ESC is also validated by simulation.

NOMENCLATURE

R	thermal resistance	(m K W^{-1})
T_b	borehole wall temperature	(K)
T_f	fluid temperature	(K)
q	heat flows per unit length	(W m^{-1})
r_{pi}	inner radius of pipe	(m)
r_p	outer radius of pipe	(m)
r_b	borehole radius	(m)
D	the half spacing of U-tube shanks	(m)
h	convective heat transfer coefficient	(W m^{-1}K^{-1})
k	thermal conductivity	(W m^{-1}K^{-1})
L_{Bor}	borehole vertical length	(m)
M	mass	(kg)
C_p	fluid specific heat	(J kg^{-1}K^{-1})
n	element number	(-)
ρ	fluid density	(kg m^{-3})
m	mass flow rate	(kg s^{-1})
T_{ran}	range temperature	(K)
P	power consumption	(W)
y	relative air flow rate	(-)
η_{car}	Carnot effectiveness	(-)
T_{eva}	evaporator temperature	(K)
T_{con}	condenser temperature	(K)

Subscript

1, 2	pipe number
in	inlet
w	water
fan	fan power
nom	nominal condition
b	grouting material
p	pipe material
f	fluid

REFERENCES

[1] H. Yang, P. Cui, Z. Fang, Vertical-borehole ground-coupled heat pumps: a review of models and systems, Appl Energy, 87 (1) (2010), pp.16-27

[2] Phetteplace, G. W. Sullivan, Performance of hybrid ground-coupled heat pump systems, ASHRAE Transactions, 104(1b) (1998), pp.763-770.

[3] M. Alavy, H.V. Nguyen, W.H. Leong, S.B. Dworkin, A methodology and computerized approach for optimizing hybrid ground source heat pump system design, Renewable Energy, 57 (2013), pp.404-412

[4] Caneta Research, Inc. *Commercial/institutional ground source heat pump engineering manual*. Atlanta: American Society of Heating, Refrigerating and Air Conditioning Engineers, Inc. (1995)

[5] S.P. Kavanaugh, K.R. Rafferty, Ground-source heat pumps: design of geothermal systems for commercial and institutional buildings, ASHRAE (1997)

[6] Kavanaugh, S.P. A design method for hybrid ground source heat pumps. ASHRAE Transactions, 104(2) (1998), pp. 691-698.

[7] A.D. Chiasson, C.C. Yavuzturk, D.W. Johnson, T.P. Filburn, Optimization of the Ground Thermal Response in Hybrid Geothermal Heat Pump Systems, ASHRAE Transactions, 116 (2010), pp.512-524

[8] L. Ni, W. Song, F. Zeng, Y. Yao, Energy saving and economic analyses of design heating load ratio of ground source heat pumps with gas boiler as auxiliary heat source, Conference on Electric Technology and Civil Engineering (ICETCE) (2011), pp. 1197-1200 [Lushan, China]

[9] Yavuzturk, C. J.D. Spitler. A short time step response factor model for vertical ground-loop heat exchangers. ASHRAE Transactions, 105(2) (1999). 475-485

[10] Yavuzturk, C. J.D. Spitler, Comparative study to investigate operating and control strategies for hybrid ground source heat pump systems using a short time-step simulation model. ASHRAE Transactions, 106 (2) (2000), pp. 192-209.

[11] Ramamoorthy, M., H. Jin, A. Chiasson, and J.D. Spitler. Optimal sizing of hybrid ground-source heat pump systems that use a cooling pond as a supplemental heat rejecter-A system simulation approach. ASHRAE Transactions, 107(1) (2001), pp. 26-38.

[12] Wrobel, J. Predictive model and application of a hybrid GSHP system for space conditioning, water heating and deicing of a seniors independent living center. Proceedings of 2004 ASME International Mechanical Engineering Congress and Exposition, Anaheim, CA. (2004)

[13] Hackel, S. P. Development of design guidelines for hybrid ground-coupled heat pump systems. ASHRAE TRP-1384 Final Report. Atlanta: American Society of Heating, Refrigerating and Air-Conditioning Engineers, Inc. (2008)

[14] Man, Y., Yang, H. and Fang Z. "Study on hybrid ground-coupled heat pump systems," *Energy and Buildings*, 40 (2008), pp. 2028-2036

[15] K.B. Ariyur and M. Krstić, *Real-Time Optimization by Extremum-Seeking Control*, John Wiley & Sons, Inc, New York, NY, 2003

[16] M. Krstić, Performance improvement and limitations in extremum seeking control, Systems and Control Letters, 39 (5) (2000), pp.313-326

[17] M. Krstić and H.-H. Wang, Stability of extremum seeking feedback for general nonlinear dynamic systems, Automatica, 36 (4) (2000), pp.595-601

[18] P. Li, Y. Li, J.E. Seem, Efficient operation of air-side economizer using extremum seeking control, Journal of Dynamic Systems, Measurement and Control, 132(3) (2010) 10, 031009

[19] X. Li, Y. Li, J.E. Seem, Dynamic modeling of mechanical draft counter-flow wet cooling tower with modelica, in: Proceedings of the 4th National Conference of IBPSA-USA, New York City, NY, 2010, pp. 193-200

[20] Modelica Association, Modelica and Modelica Association, 2014. http://www.modelica.org

[21] Lawrence Berkeley National Laboratory, Modelica Library for Building Energy and Control Systems, 2014. http://simulationresearch.lbl.gov/modelica

[22] H.Y. Zeng, N.R. Diao, Z.H. Fang, Efficiency of vertical geothermal heat exchangers in ground source heat pump systems, J. Thermal Sci. 12 (1) (2003), pp.77–81

[23] H.Y. Zeng, N.R. Diao, Z.H. Fang, Heat transfer analysis of boreholes in vertical ground heat exchangers [J], International Journal of Heat and Mass Transfer, 46(23) (2003), pp.4467–4481

[24] J.D. Deerman, S.P. Kavanaugh, Simulation of vertical U-tube ground coupled heat pump systems using the cylindrical heat source solution, ASHRAE Trans, 97 (1) (1991), pp. 287–295

[25] EnergyPlus, Engineering Reference, October 1, 2013, http://apps1.eere.energy.gov/buildings/energyplus/energyplus_documentation.cfm

[26] M.A. Rotea, Analysis of multivariable extremum seeking algorithms, in: Proceedings of American Control Conference, Chicago, IL, 2000, pp. 433-437

[27] X. Li, Y. Li, J. E. Seem, P. Li, Dynamic modeling and self-optimizing operation of chilled water systems using extremum seeking control, Energy and Buildings, 58 (2013), pp.172-182

[28] Y. Peng, D. Vrancic, R. Hanus, Anti-windup, bumpless, and conditioned transfer techniques for PID controllers, IEEE Control Systems Magazine, 16(4) (1996), pp.48-57

[29] P. March, M. Turner, Anti-windup compensator designs for nonsalient permanent-magnet synchronous motor speed regulators, IEEE Transactions on Industry Applications, 45(5) (2009), pp.1598-1609.

[30] Y. Li, J.E. Seem, Extremum seeking control with actuator saturation control, US Patent, 20100106331, 2010.